DOI: 10.13208/j.electrochem.191228
Cite this: *J. Electrochem.* **2020**, *26*(6): 797-807

Article ID:1006-3471(2020)06-0797-11
Http://electrochem.xmu.edu.cn

Effect of Reaction Conditions on Cu-Catalyzed CO_2 Electroreduction

ZHU Chang[1,2], CHEN Wei[1]*, SONG Yan-fang[1], DONG Xiao[1], LI Gui-hua[1], WEI Wei[1,3*], SUN Yu-han[1,3*]

((1. *CAS Key Laboratory of Low-carbon Conversion Science and Engineering, Shanghai Advanced Research Institute, Chinese Academy of Sciences, Shanghai*, 201210, *China*; 2. *University of Chinese Academy of Sciences, Beijing*, 100049, *China*; 3. *School of Physical Science and Technology, ShanghaiTech University, Shanghai*, 201210, *China*)

Abstract: Electrochemical conversion of carbon dioxide (CO_2) driven by renewable electricity that can meet both carbon emission reduction and renewable energy utilization has been rapidly developed in recent years. Copper (Cu) catalyst has long been a promising candidate for CO_2 electroreduction applications because of its natural abundance and specific capability of producing a substantial amount of C2 products. However, various metallic Cu electrodes reported have been significantly influenced by the adsorption of certain cation/anion ions, resulting in wide-span catalytic activities and selectivity for various products. In addition, a recent report demonstrated that by virtue of gas-diffusion flow cell with Cu cathode, remarkable ethylene production was achieved in CO_2 electroreduction. It is, therefore, desirable to systematically investigate the effect of reaction conditions on the performances of Cu-catalyzed CO_2 electroreduction. Here we chose the commercial Cu particles with an average size of 600 nm as the catalyst for CO_2 electroreduction and investigated the electrocatalytic performances under various reaction conditions, including the commonly used electrolyte solutions, the different potassium hydrogen carbonate ($KHCO_3$) concentrations, as well as H-type and gas-diffusion flow cells. The results of linear sweep voltammetry and potentiostatic CO_2 electrolysis showed that $KHCO_3$ as an electrolyte solution with a concentration of 0.5 mol·L^{-1} offered good catalytic activities and high current densities, and the gas-diffusion flow cell could further improve the Faradaic efficiencies and partial current densities of the main products formate and CO. This work provides a fundamental insight to the electrocatalytic conversion of CO_2 reduction from the view of reaction conditions.

Key words: CO_2 electroreduction; copper catalyst; reaction conditions; gas-diffusion electrode

CLC Number: O646 **Document Code:** A

Ever-increasing atmospheric level of carbon dioxide (CO_2) caused by industry-scale fossil energy consumption has threatened global sustainable development. It is expected that the utilization of CO_2 will become increasing concerns in the near future with stricter policies and ambitious prospects on carbon emission reduction worldwide[1-5]. The conversion of CO_2 into value-added products remains much attracting, which could not only decrease atmospheric CO_2 levels, but also produce fuels to alleviate the energy stress partially[6-7]. Traditional catalytic processes involving CO_2 conversion to useful chemicals/fuels include industrial methanol synthesis, methane or water/CO_2 reforming, reverse water gas shift reaction, and syntheses of organic acids/esters with CO_2 [8-10]. Although these catalytic reactions have a certain impact on reducing the net increase of CO_2 emission, the current technologies require relatively hard conditions of high temperature, high pressure and an equivalent amount of hydrogen as the reducing agent. This means high energy consumption and more valuable hydrogen involved to realize such CO_2

Received: 2019-12-30, Revised: 2020-02-25. *Corresponding author, Tel: (86-21)20608005, E-mail: chenw@sari.ac.cn; weiwei@sari.ac.cn; sunyh@sari.ac.cn

conver sion by the traditional thermocatalytic pathways[11-12]. Furthermore, complicated reactors and complete infrastructures are invested in advance to run the above reactions. In comparison, electrochemical reduction of CO_2 is a preferred alternative way, which can produce CO, hydrocarbon or oxygenates utilizing low-grade electrical energy from intermittent renewable energy sources such as solar, wind, etc.[13-16].

Extensive metal electrodes have been investigated for electrocatalytic CO_2 conversion, and copper (Cu) distinguished itself from other metal electrodes due to its unique properties of capable of producing multicarbon compounds, which has been mostly studied and can be considered as a promising electrode material with low cost and natural abundance for electrocatalytic CO_2 reduction[17-20]. As early as 1985, Hori et al.[21] reported that the electrochemical reduction of CO_2 over Cu electrode in an aqueous solution can produce substantive methane (CH_4) and ethylene (C_2H_4), as well as trace ethanol (C_2H_5OH, EtOH) and n-propanol (C_3H_7OH, n-PrOH). A large number of studies on CO_2 electroreduction have been widely carried out with Cu electrodes to further improve their electrocatalytic performances. The product distributions and Faradaic efficiencies (FEs) of Cu-catalyzed CO_2 electroreduction were largely affected by the type and concentration of electrolyte. For instance, C_2H_4 and alcohols would be the main products in KCl, K_2SO_4 and low-concentration HCO_3- solutions, while the formation of CH_4 was preferred in high-concentration HCO_3^- electrolyte[22]. Jiao et al.[23] reported the activities of CO_2 electroreduction over the porous Cu electrode followed the electrolyte conductivity variance trends with KOH > KCl > K_2SO_4 > $KHCO_3$. The diverse preferred cation and anion ions adsorbed on the Cu electrode led to distinct CO_2 activation and intermediate evolution kinetics, which are responsible for such product distributions and selectivity[24]. In addition, more studies have focused on gas diffusion electrodes (GDEs) in the flow cell in recent years, in which the diffusion behaviors of the reactants/products over Cu catalyst surface were facilitated, resulting in higher CO_2 conversion rate and current efficiency[25-27]. Sargent et al.[28] reported a stable ethylene FE of 70% (-0.55V vs. RHE, 750 mA·cm^{-2}) with Cu electrode for electroreduction CO_2 under strongly alkaline 10 mol·L^{-1} KOH in the flow cell. While the ethylene FE could reach 60% at the current density of only 12 mA·cm^{-2} in H-type cell over plasma oxidized Cu electrodes reported by Hemma et al.[29].

Since Cu catalysts showed quite broad electrocatalytic performances of CO_2 reduction under various reaction conditions, it is desirable to systematically investigate the effect of reaction conditions on the performances of Cu-catalyzed CO_2 electroreduction. Herein, commercially available 600 nm spherical Cu particles were used as the electrocatalyst to exclude the possible influences derived from nano size effect, shape, etc.[30]. The electrolyte salts commonly used in chemistry were chosen as electrolyte solutions, and the appropriate electrolyte ($KHCO_3$) was determined for subsequent reaction condition studies based on its optimal CO_2 performances. The different concentrations of $KHCO_3$ and types of the electrolysis cells were further tested for acquiring optimal reaction conditions for CO_2 electroreduction.

1 Experimental Section

1.1 Chemicals

Commercially available copper powder (~ 600 nm) was purchased from Shanghai Xiangtian Nano Materials Co. Ltd. Potassium hydrogen carbonate ($KHCO_3$), sodium hydrogen carbonate ($NaHCO_3$), potassium sulfate (K_2SO_4), sodium sulfate (Na_2SO_4), lithium sulfate (Li_2SO_4), potassium chloride (KCl), sodium chloride (NaCl), and lithium chloride (LiCl), all of analytical grade, were purchased from Sino Pharm Chemical Reagent Co. Ltd. All solutions were prepared, and all glassware was cleaned by using deionized water (Master-S30UVF, 18.2 MΩ).

1.2 Characterizations

TEM images were obtained on a Titan ST microscope (FEI Co.) operated at an accelerating voltage of 300 kV. XRD patterns of the catalysts were obtained on a Rigaku Ultima 4 X-ray diffractometer utilizing Cu K_α radiation (λ = 1.54056 Å) under 40

kV, 40 mA and scanning speed of 4 °·min^{-1}. XPS spectra were obtained by an X-ray photoelectron spectrometer (Quantum 2000 Scanning ESCA Microprobe instrument) with a monochromatic excitation source of Al K_α radiation ($h\nu$ = 1486.6 eV) performed under 12 kV and 4 mA. The peaks of Cu 2p and Cu LMM auger were recorded in the binding energy ranges of 925 ~ 965 eV and 555 ~ 585 eV, respectively. The binding energies in all XPS spectra were calibrated according to the C 1s peak (284.8 eV). The XPS spectra were deconvoluted by using a commercially available data-fitting program (Thermo Advantage software) after a Shirley background subtraction procedure.

1.3 Electrochemical Measurements

The electrocatalytic activities of the catalysts were measured using a gas-tight electrolysis cell and a Biologic VMP3 potentiostat. A KCl-saturated Ag/AgCl electrode and a Pt wire were used as the reference and counter electrodes, respectively. The carbon paper coated with Cu particles was used as the working electrode. The working and counter electrode compartments were separated using a proton exchange membrane (Nafion 117, Dupont). The aqueous solutions consisted of different electrolyte salts were used as the electrolyte (40 mL in each compartment), and saturated with CO_2 (99.999%, the pH value of the saturated solution was measured to be 7.2). CO_2 was delivered into the cathodic compartment (outlet directly connected to the GC) at a constant rate of 10 mL·min^{-1} and was allowed to purge for 60 min prior to the experiments. The linear sweep voltammetry (LSV) curves were obtained at a scan rate of 10 mV·s^{-1}. The tests of the potentiostatic CO_2 electrolysis were conducted at various potentials for electrocatalytic performance comparison. All of the applied potentials were recorded against Ag/AgCl (saturated KCl) reference electrode and then converted to reversible hydrogen electrode (RHE) using E(vs. RHE) = E (vs. Ag/AgCl) + 0.197 V + 0.0591 × pH. Gas products from the cathodic compartment during the electrochemical reactions were analyzed using a GC-2014 (Shimadzu) equipped with a Molecular sieve-13X 60/80 column and a Plot-Q80/100 column. Liquid products were analyzed using another off-line GC-2014 (Shimadzu) equipped with an autosampler and an OVI-G43 capillary column (Supelco, USA). Formate in liquid products was analyzed by using a 600 MHz NMR spectrometer (Bruker), with DSS and D_2O as internal standards.

2 Results and Discussion

2.1 Morphologies and Phase/Surface Compositions of Cu Particles

The surface morphologies and phase/surface compositions of Cu particles are shown in Fig. 1. The SEM image (Fig. 1A) shows the spherical Cu particles with an average diameter of about 600 nm (Fig. 1B). The XRD pattern of Cu particles (Fig. 1C) indicates that all diffraction peaks are indexed to metallic Cu (111), (200), and (220) planes (JCPDS No. 040836). The HRTEM analysis (Fig. 1D) shows that the fringes of these granules are metallic copper phase, with a lattice spacing of 2.08 Å corresponding to the Cu[111] plane. Both the XPS spectrum (Fig. 1E) and the Auger spectrum (Fig. 1F) confirm that the surface composition of Cu particles is metallic Cu.

2.2 Effect of Electrolyte Variety

Because the partial current density and overpotential, which indicate the capability of obtaining products[31-32], are important in CO_2 electroreduction, the LSV curves were used to firstly screen the electrolytes. Fig. 2 shows the LSV curves of Cu particles in various CO_2-saturated electrolyte solutions. One sees that the current density in K_2SO_4 was the largest compared to other electrolyte solutions in the potential range from 0 to -1.4 V (vs. RHE). This may be attributed to two aspects: (1) the conductivities of the cation ions show the order of $K^+ > Na^+ > Li^+$; (2) divalent anion ion SO_4^{2-} possesses the greater ionic strength, as recognized previously. The solutions of LiCl and $NaHCO_3$ showed the low current densities with the narrow potential range from -0.6 to -1.4 V (vs. RHE). In addition, the broad peak around -0.4 V (vs. RHE) in the LSV curve of K_2SO_4 may be attributed to the hydrogen evolution (vide infra). The electrolytes of Na_2SO_4, KCl, Li_2SO_4, $KHCO_3$ and Na-

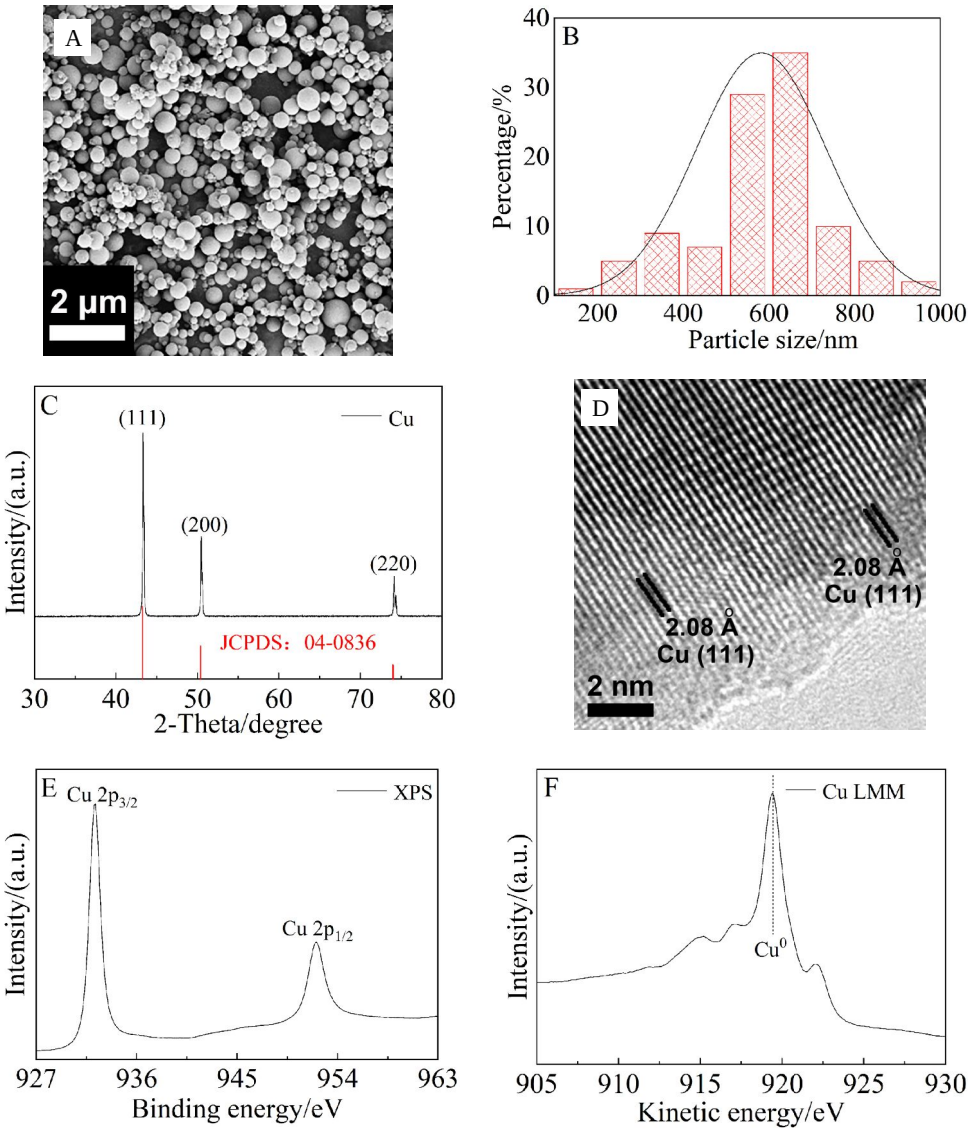

Fig. 1 (A) SEM image, (B) size distribution, (C) XRD pattern, (D) HRTEM image, (E) XPS spectrum of Cu 2p, and (F) Auger spectrum of Cu LMM for Cu particles.

Cl had almost the same potential windows from -0.3 to -1.4 V (vs. RHE) and similar current densities. The current densities of LiCl and $NaHCO_3$ were the smallest among the tested electrolytes, implying their inferior capabilities for CO_2 electroreduction. From the perspectives of the current density and electrochemical window, the above electrolytes except for LiCl and $NaHCO_3$ are appropriate for aqueous CO_2 electroreduction in principle.

The electrocatalytic performances of CO_2 reduction over Cu particles in different electrolyte solutions are shown in Fig. 3. Apparently, formate and H_2 were the main products in all electrolyte solutions, accompanying with the other products such as CO, CH_4, C_2H_4, EtOH and n-PrOH. H_2 is derived from the competitive hydrogen evolution reaction (HER) and the suppression of HER is always one of the important goals in CO_2 electroreduction studies. The FEs (Fig. 3A) and the partial current densities (Fig. 3B) in all products suggested only in three electrolyte solutions of $NaHCO_3$, KCl and $KHCO_3$ preferred the formation of formate to that of H_2. Moreover, the products from CO_2 reduction reached their maximum, while H_2 formation was greatly suppressed in $KHCO_3$

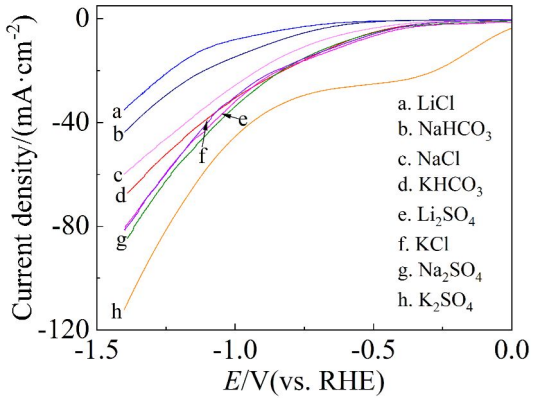

Fig. 2 LSV curves obtained in different CO_2 saturated electrolyte solutions with a concentration of 0.5 mol·L^{-1} (scan rate 10 mV·s^{-1}).

solution, indicating that $KHCO_3$ is the best electrolyte for CO_2 electroreduction. Furthermore, the CO_2 electroreduction performances in KCl solution were much better than those in $NaHCO_3$, implying that the reactant is the dissolved CO_2 molecules rather than HCO_3^- anions, in agreement with the previous reports[33]. Note that H_2 FEs in both NaCl and KCl solutions were lower than those in Na_2SO_4 and K_2SO_4 solutions, which can be attributed to the adsorbed Cl^- on Cu particle surface hindering HER. The adsorption of Cl^- on the Cu electrode surface had benn recognized previously[34-35], and the improvement of catalytic performance was mainly due to the specific Cl^- adsorption on the copper surface, which facilitates the formation and stabilization of carboxyl (*COOH) intermediates by the partial charge contribution of Cl^-. On the contrary, the small cation Li^+ decreased the preferred adsorption of Cl^- due to the ion-pairing effect[36], resulting in the reversed H_2 formation in LiCl solution compared to Li_2SO_4 solution. Furthermore, the presence of Cl^- in the anodic compartment may induce the occurrence of Cl_2 evolution reaction, thus, the electrolyte solutions including Cl^- are not appropriate for CO_2 electroreduction. On the other hand, although K_2SO_4 possesses the highest conductivity and current density in LSV (Fig. 2) among all the tested electrolytes, the corresponding H_2 FE was as high as 55%, while the formate FE was only about 45%, as well as the other products from CO_2 reduction were almost negligible, which indicate the inferior activities of CO_2 electroreduction in K_2SO_4 solution. The reason of high H_2 FE in K_2SO_4 solution might be the absence of the specific adsorption and the non-equilibrium local region of high pH near the electrode[23,37]. Therefore, the criterion of electrolyte should be based on the capacities of reducing CO_2 and suppressing HER, and the high ionic conductivity is not a key factor because the formation of H_2 may also be facilitated.

2.3 Effect of Electrolyte Concentration

The effect of electrolyte concentration in

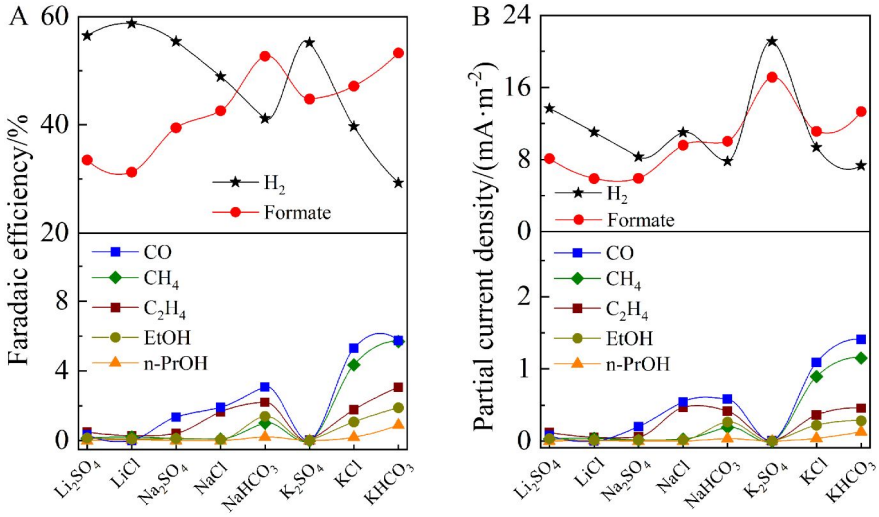

Fig. 3 (A) Faradaic efficiency and (B) partial current density of products over Cu particles in different CO_2-saturated electrolyte solutions (0.5 mol·L^{-1}) at -1.0 V vs. RHE.

$KHCO_3$ on CO_2 electroreduction was further studied. Fig. 4 shows the LSV curves of Cu particles in various CO_2-saturated $KHCO_3$ solutions with the concentrations from 0.05 mol·L^{-1} to 2.0 mol·L^{-1}. From the LSV curves in both Fig. 2 and Fig. 4, the current densities rapidly increased after -1.0 V vs. RHE, implying the transition of kinetic control to mass transfer, in agreement with the previous reports[38-39]. The current densities increased with increasing $KHCO_3$ concentrations, accompanying gradually positive shift onset potentials (Fig. 4). High current densities in higher concentrations of $KHCO_3$ solutions are derived from the increasing ionic conductivity of electrolyte. Fig. 5A shows the FEs of H_2 and other products from CO_2 reduction in $KHCO_3$ solutions with different concentrations. The H_2 FE was 38% in 0.05 mol·L^{-1} $KHCO_3$, and stepwise decreased with increasing concentrations and reached the minimum (29%) in 0.5 mol·L^{-1} $KHCO_3$. It is interesting that the FE of H_2 increased from 0.5 mol·L^{-1} to 2.0 mol·L^{-1}, indicating that HER was facilitated in $KHCO_3$ solutions with higher concentrations. Formate is always the main product and its FE fluctuates in the range of 40% ~ 52% in the different concentrations of $KHCO_3$ solutions. The CO FEs monotonously decreased with increasing $KHCO_3$ concentrations that are attributed to the competitions from HER and other CO_2 reduction

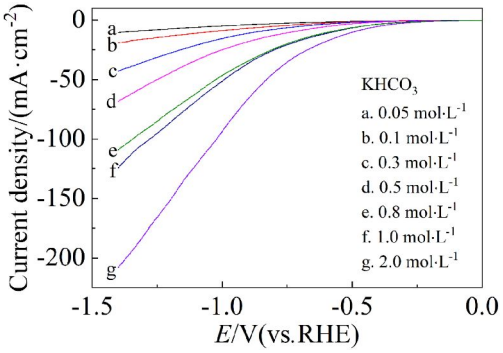

Fig. 4 LSV curves obtained in the CO_2-saturated $KHCO_3$ solutions with different concentrations (scan rate 10 mV·s^{-1}).

pathways, in which adsorbed CO is considered as the key intermediates for further C-C coupling or/and proton-electron transfer to form various products[40-41].

The FEs of CH_4, C_2H_4 and EtOH had a similar variant tendency, i.e., these FEs increased from 0.05 mol·L^{-1} to 0.5 mol·L^{-1}, then decreased gradually with increasing $KHCO_3$ concentrations. And the FE of n-PrOH reached the maximum in 0.3 mol·L^{-1} $KHCO_3$ solution, a little ahead compared to those of CH_4, C_2H_4 and EtOH. Although the partial current densities of formate and H_2 increased with increasing $KHCO_3$ concentrations (Fig. 5B), the formate partial current density showed a leap from 0.3 to 0.5 mol·L^{-1} $KHCO_3$. Moreover, all the other products possessed the maxi-

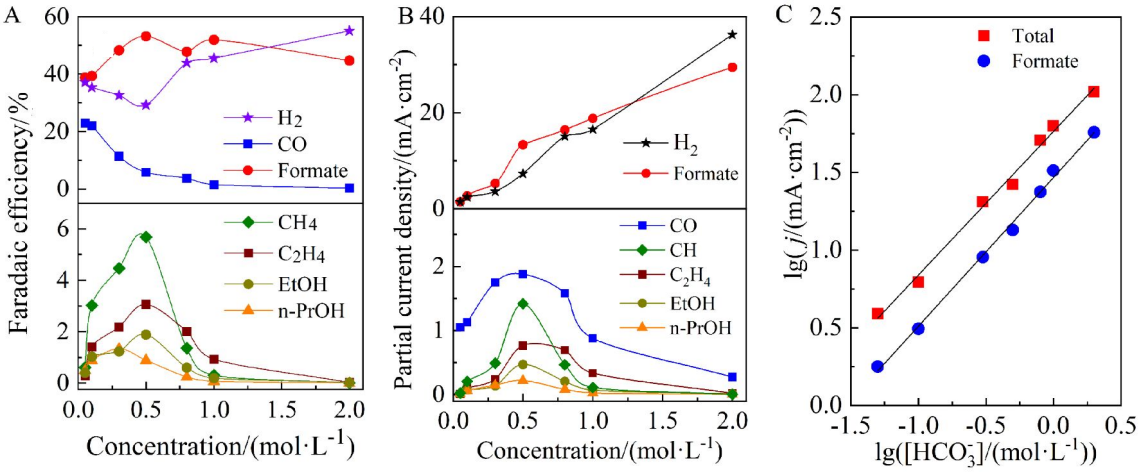

Fig. 5 (A) Faradaic efficiencies and (B) partial current densities of products over Cu particles in different CO_2-saturated $KHCO_3$ solutions with the concentrations from 0.05 mol·L^{-1} to 2.0 mol·L^{-1} at -1.0 V vs. RHE. (C) Total and formate partial current densities versus $KHCO_3$ concentrations.

mum partial current densities in 0.5 mol·L^{-1} $KHCO_3$ solution (Fig. 5B). Fig. 5C shows the linear relationships between the concentration of $KHCO_3$ and the total current density or the main product (formate) partial current density, indicating that CO_2 electroreduction in $KHCO_3$ aqueous solution is a first-order reaction as reported previously[42-44]. With 0.5 mol·L^{-1} concentration of $KHCO_3$ aqueous solution, the H_2 partial current density was relatively low, while the partial current densities of CO_2 reduction products were in the optimal levels, indicating that the concentration of 0.5 mol·L^{-1} is beneficial for inhibiting HER and promoting CO_2 electroreduction.

2.4 Effect of Reaction Systems

In traditional H-type cells, CO_2 dissolved in the aqueous cathodic electrolyte solution was reduced to various products on the catalyst surface, in which the limitations of CO_2 solubility and mass transfer caused the ordinary electrochemical performances. These issues can be well solved with a gas diffusion electrode in a flow electrolysis cell, resulting in high current density and energy efficiency. In general, CO_2 reactant does not directly contact the electrolyte solution due to the separation of hydrophobic polymer-based gas diffusion interface, so high-concentration stronger alkali solutions are frequently used in flow electrolysis cells[45-46]. For comparison, the tested electroreduction reaction systems include 0.5 mol·L^{-1} $KHCO_3$ solution in H-type cell and flow cell, as well as 0.5 mol·L^{-1} KOH and 1.0 mol·L^{-1} KOH in the flow cell, which are denoted as H-0.5 mol·L^{-1} $KHCO_3$, F-0.5 mol·L^{-1} $KHCO_3$, F-0.5 mol·L^{-1} KOH and F-1.0 mol·L^{-1} KOH, respectively. The LSV curves under these reaction systems are shown in Fig. 6. One sees that the current density of F-0.5 mol·L^{-1} $KHCO_3$ was larger than that of H-0.5 mol·L^{-1} $KHCO_3$ though they possessed the similar onset potentials, implying the better mass-transfer ability in the flow cell. When the electrolyte of flow cell was changed from $KHCO_3$ to KOH, the current density was further increased accompanying the positive shift of onset potential about 0.2 V. This is attributed to the lower resistance of electrolyte solution for the higher conductivity of

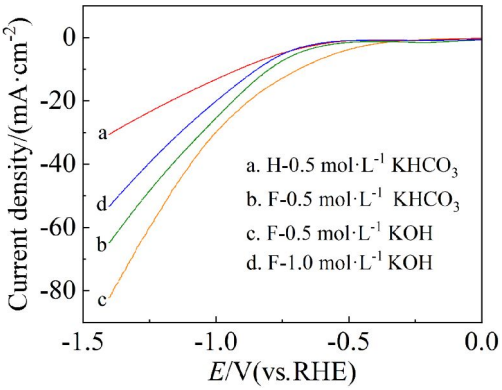

Fig. 6 LSV curves obtained under different reaction systems (scan rate 10 mV·s^{-1}).

KOH solution. It is interesting that the increase of KOH concentration from 0.5 mol·L^{-1} to 1.0 mol·L^{-1} resulted in a negatively shifted onset potential, though the current density in 1.0 mol·L^{-1} KOH was larger than that in 0.5 mol·L^{-1} KOH. A similar phenomenon was also reported by Sargent, which was the result of the CO_2 reduction kinetic variety in high-concentration hydroxide-mediated interface [47]. That is why the initial potential of CO_2 electroreduction shifts significantly to a more positive potential as increasing KOH concentrations, resulting in the hampered occurrence of the competing hydrogen evolution reaction. At the same time, the CO_2 molecules easily accumulated at the high-concentration hydroxide-mediated interface also improved the kinetic of CO_2 reduction[28].

The FEs and partial current densities of products over Cu particles in different reaction systems are shown in Fig. 7. For all reaction systems, H_2 and formate were main products with the FEs of 28% ~ 32% and 54% ~ 60%, respectively, followed by CO and other minor products C_2H_4, CH_4, EtOH and n-PrOH (Fig. 7A). Formations of formate and CO in flow cell are preferred to those in H-type cell comparing with H_2 formation. Moreover, the high-concentration KOH in flow cell can further facilitate CO formation and suppress H_2 formation. Furthermore, Sargent and co-authors reported the home-fabricated copper gas diffusion electrode with the special graphite/carbon NPs/Cu/PTFE configuration, which played a vital

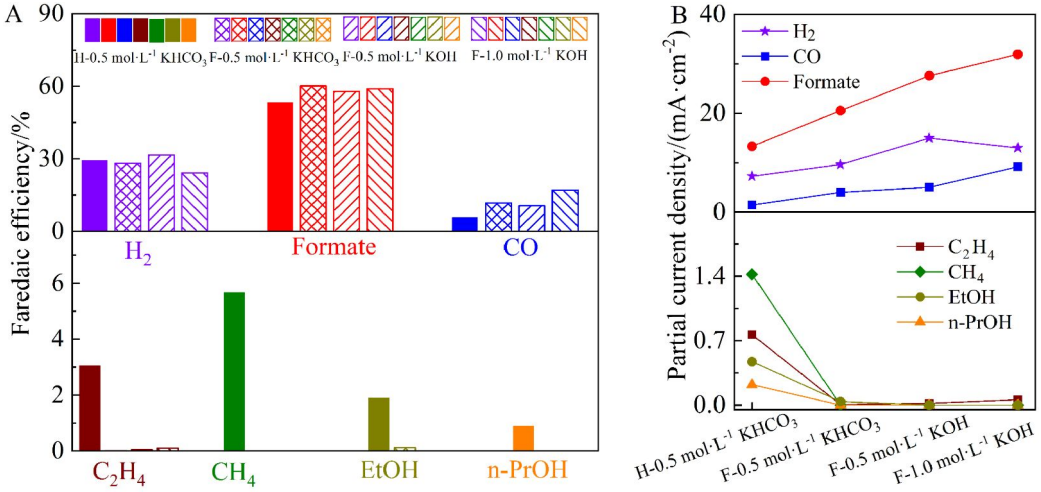

Fig. 7 (A) Faradaic efficiencies and (B) partial current densities of products over Cu particles in different CO_2 electroreduction reaction systems at -1.0 V vs. RHE.

role for producing complex products such as C_2H_4, CH_4 and alcohols[28]. The copper electrode configuration in flow cell is not delicate enough, resulting in the inferior formations of C_2H_4, CH_4 and alcohols in flow cell. The partial current densities of formate and CO showed the orders of H-0.5 mol·L^{-1} $KHCO_3$ < F-0.5 mol·L^{-1} $KHCO_3$ < F-0.5 mol·L^{-1} KOH < F-1.0 mol·L^{-1} KOH, while the partial current densities of other CO_2 reduction products in flow cell were negligible (Fig. 7B).

3 Conclusions

In summary, this work systematically investigated the effects of various reaction conditions including electrolyte varieties, electrolyte concentrations and reaction systems on CO_2 electroreduction with commercial Cu particles as electrocatalysts. Although the electrolytes with larger cations such as Cs^+ and methyl ammonium showed the comparable performance in CO_2 electroreduction[48-49], which were excluded here considering the electrolyte availability and stability. Based on the perspectives of Faradaic efficiency and partial current density of products, as well as the exclusion of possible harmful side reaction (such as chlorine evolution reaction), $KHCO_3$ was considered as the best electrolyte for aqueous CO_2 electroreduction, and the appropriate $KHCO_3$ concentration (0.5 mol·L^{-1}) was beneficial for facilitating CO_2 reduction and suppressing HER. And the flow cell could further improve the electrochemical performance of CO_2 reduction with both higher Faradaic efficiencies and partial current densities of formate and CO. This work provides a general recognition about the effects of reaction conditions on the performances of CO_2 electroreduction.

Acknowledgements

This work was supported by the National Natural Science Foundation of China (Nos. 91745114, 21802160), the Ministry of Science and Technology of China (Nos. 2016YFA0202800, 2018YFB0604700), Shanghai Sailing Program (No. 18YF1425700), Shanghai Advanced Research Institute Innovation Research Program (Nos. Y756812ZZ1 and Y756803ZZ1), and Shanghai Functional Platform for Innovation Low Carbon Technology. W. C. also acknowledges the support from the Hundred Talents Program of Chinese Academy of Sciences.

References:

[1] Caldeira K, Wickett M E. Anthropogenic carbon and ocean pH[J]. Nature, 2003, 425(6956): 365.

[2] White J W C, Ciais P, Figge R A, et al. A high-resolution record of atmospheric CO_2 content from carbon isotopes in peat[J]. Nature, 1994, 367(6459): 153-156.

[3] Chu S, Majumdar A. Opportunities and challenges for a sustainable energy future[J]. Nature, 2012, 488(7411):

294-303.

[4] Obama B. The irreversible momentum of clean energy [J]. Science, 2017, 355(6321): 126-129.

[5] Zhang X R(张旭锐), Shao X L(邵晓琳), Yi J(易金), et al. Statuses, Challenges and strategies in the development of low-temperature carbon dioxide electroreduction technology[J]. Journal of Electrochemistry(电化学), 2019, 25 (4): 413-425.

[6] Wang L M, Chen W L, Zhang D D, et al. Surface strategies for catalytic CO_2 reduction: from two-dimensional materials to nanoclusters to single atoms[J]. Chemical Society Reviews, 2019, 48(21): 5310-5349.

[7] Song R B, Zhu W, Fu J, et al. Electrode materials engineering in electrocatalytic CO_2 reduction: Energy input and conversion efficiency[J]. Advanced Materials, 2019, 32(27): 1903796.

[8] Askgaard T S, Norskov J K, Ovesen C V, et al. A kinetic model of methanol synthesis[J]. Journal of Catalysis, 1995, 156(2): 229-242.

[9] Iglesias M L, de Vries C, Claeys M, et al. Chemical energy storage in gaseous hydrocarbons via iron Fischer-Tropsch synthesis from H_2/CO_2 Kinetics, selectivity and process considerations[J]. Catalysis Today, 2015, 242: 184-192.

[10] Liu J J, Peng H G, Liu W M, et al. Sn modification on Ni/Al_2O_3: Designing potent coke-resistant catalysts for methane dry reforming[J]. Chemcatchem, 2014, 6(7): 2095-2104.

[11] Birdja Y Y, Pé rez-Gallent E, Figueiredo M C, et al. Ad vances and challenges in understanding the electrocatalytic conversion of carbon dioxide to fuels[J]. Nature Energy, 2019, 4(9): 732-745.

[12] Zhou W, Cheng K, Kang J C, et al. New horizon in C1 chemistry: breaking the selectivity limitation in transformation of syngas and hydrogenation of CO_2 into hydrocarbon chemicals and fuels[J]. Chemical Society Reviews, 2019, 48(12): 3193-3228.

[13] Liu M, Pang Y J, Zhang B, et al. Enhanced electrocatalytic CO_2 reduction via field-induced reagent concentration [J]. Nature, 2016, 537(7620): 382-386.

[14] Bai X F, Chen W, Zhao C C, et al. Exclusive formation of formic acid from CO_2 electroreduction by a tunable Pd-Sn alloy[J]. Angewandte Chemie International Edition, 2017, 56(40): 12219-12223.

[15] Gao S, Lin Y, Jiao X C, et al. Partially oxidized atomic cobalt layers for carbon dioxide electroreduction to liquid fuel[J]. Nature, 2016, 529(7584): 68-71.

[16] Yang F(杨帆), Deng P L(邓培林), Han Y J(韩优嘉), et al. Copper-based compounds for electrochemical reduction of carbon dioxide[J]. Journal of Electrochemistry(电化学), 2019, 25(4): 426-444.

[17] Lim D H, Jo J H, Shin D Y, et al. Carbon dioxide conversion into hydrocarbon fuels on defective graphene supported Cu nanoparticles from first principles[J]. Nanoscale, 2014, 6(10): 5087-5092.

[18] Keerthiga G, Viswanathan B, Chetty R. Electrochemical reduction of CO_2 on electrodeposited Cu electrodes crystalline phase sensitivity on selectivity[J]. Catalysis Today, 2015, 245: 68-73.

[19] Chen C S, Handoko A D, Wan J H, et al. Stable and selective electrochemical reduction of carbon dioxide to ethylene on copper mesocrystals[J]. Catalysis Science & Technology, 2015, 5(1): 161-168.

[20] Lei W(雷文), Xiao W P(肖卫平), Wang D L(王得丽), et al. Recent progress in copper-based catalysts for electrochemical CO_2 reduction[J]. Journal of Electrochemistry (电化学), 2019, 25(4): 455-466.

[21] Hori Y, Kikuchi K, Suzuki S. Production of CO and CH_4 in electrochemical reduction of CO_2 at metal-electrodes in aqueous hydrogencarbonate solution[J]. Chemistry Letters, 1985, 14: 1695-1698.

[22] Hori Y, Murata A, Takahashi R. Formation of hydrocarbons in the electrochemical reduction of carbon dioxide at a copper electrode in aqueous solution[J]. Journal of the Chemical Society, Faraday Transactions 1: Physical Chemistry in Condensed Phases, 1989, 85(8): 2309-2326.

[23] Lv J J, Jouny M, Luc W, et al. A highly porous copper electrocatalyst for carbon dioxide reduction[J]. Advanced Materials, 2018, 30(49): 1803111.

[24] Garza A J, Bell A T. Head-Gordon M. Mechanism of CO_2 reduction at copper surfaces: Pathways to C_2 products[J]. ACS Catalysis, 2018, 8(2): 1490-1499.

[25] Ren S X, Joulie D, Salvatore D, et al. Molecular electrocatalysts can mediate fast, selective CO_2 reduction in a flow cell[J]. Science, 2019, 365(6451): 367-369.

[26] Salvatore D A, Weekes D M, He J, et al. Electrolysis of gaseous CO_2 to CO in a flow cell with a bipolar membrane[J]. ACS Energy Letters, 2017, 3(1): 149-154.

[27] Weng L C, Bell A T, Weber A Z. Modeling gas-diffusion electrodes for CO_2 reduction[J]. Physical Chemistry Chemical Physics, 2018, 20(25): 16973-16984.

[28] Dinh C T, Burdyny T, Kibria M G, et al. CO_2 electroreduction to ethylene via hydroxide-mediated copper catalysis at an abrupt interface[J]. Science, 2018, 360(6390): 783-787.

[29] Mistry H, Varela A S, Bonifacio C S, et al. Highly selective plasma-activated copper catalysts for carbon dioxide reduction to ethylene[J]. Nature Communications, 2016, 7:

12123.

[30] Reske R, Mistry H, Behafarid F, et al. Particle size effects in the catalytic electroreduction of CO_2 on Cu nanoparticles[J]. Journal of the American Chemical Society, 2014, 136(19): 6978-6986.

[31] Birdja Y Y, Pérez-Gallent E, Figueiredo M C, et al. Advances and challenges in understanding the electrocatalytic conversion of carbon dioxide to fuels[J]. Nature Energy, 2019, 4(9): 732-745.

[32] Spurgeon J M, Kumar B. A comparative technoeconomic analysis of pathways for commercial electrochemical CO_2 reduction to liquid products[J]. Energy & Environmental Science, 2018, 11(6), 1536-1551.

[33] Min X, Kanan M W. Pd-catalyzed electrohydrogenation of carbon dioxide to formate: high mass activity at low overpotential and identification of the deactivation pathway[J]. Journal of the American Chemical Society, 2015, 137(14): 4701-4708.

[34] Gao D F, Scholten F, Roldan Cuenya B. Improved CO_2 Electroreduction performance on plasma-activated Cu catalysts via electrolyte design: Halide effect[J]. ACS Catalysis, 2017, 7(8): 5112-5120.

[35] Varela A S, Ju W, Reier T, et al. Tuning the catalytic activity and selectivity of Cu for CO_2 electroreduction in the presence of halides[J]. ACS Catalysis, 2016, 6(4): 2136-2144.

[36] Irina V C, Sathish P. Activation of CO_2 at the electrode-electrolyte interface by a co-adsorbed cation and an electric field[J]. Physical Chemistry Chemical Physics, 2019, 21(17), 8797-8807.

[37] Yoon Y, Hall A S, Surendranath Y. Tuning of silver catalyst mesostructure promotes selective carbon dioxide conversion into fuels[J]. Angewandte Chemie International Edition. 2016, 55(49): 15282-15286.

[38] Zhu C Q, Wang Q N, Wu C. Rapid and scalable synthesis of bismuth dendrites on copper mesh as a high-performance cathode for electroreduction of CO_2 to formate[J]. Journal of CO_2 Utilization, 2020, 36: 96-104.

[39] Singh MR, Clark EL, Bell AT. Effects of electrolyte, catalyst, and membrane composition and operating conditions on the performance of solar-driven electrochemical reduction of carbon dioxide[J]. Physical Chemistry Chemical Physics, 2015, 17(29), 18924-18936.

[40] Kuhl K P, Cave E R, Abram D N, et al. New insights into the electrochemical reduction of carbon dioxide on metallic copper surfaces[J]. Energy & Environmental Science, 2012, 5(5): 7050-7059.

[41] Zhuang T T, Liang Z Q, Seifitokaldani A, et al. Steering post-C-C coupling selectivity enables high efficiency electroreduction of carbon dioxide to multi-carbon alcohols[J]. Nature Catalysis, 2018, 1(6): 421-428.

[42] Gao S, Sun Z T, Liu W, et al. Atomic layer confined vacancies for atomic-level insights into carbon dioxide electroreduction[J]. Nature Communications, 2017, 8: 14503.

[43] Zhao C N, Dai X Y, Yao T, et al. Ionic exchange of metal-organic frameworks to access single nickel sites for efficient electroreduction of CO_2[J]. Journal of the American Chemical Society, 2017, 139(24): 8078-8081.

[44] Dunwell M, Lu Q, Heyes J M, et al. The central role of bicarbonate in the electrochemical reduction of carbon dioxide on gold[J]. Journal of the American Chemical Society, 2017, 139(10): 3774-3783.

[45] Bitar Z, Fecant A, Trela-Baudot E, et al. Electrocatalytic reduction of carbon dioxide on indium coated gas diffusion electrodes-comparison with indium foil[J]. Applied Catalysis B - Environmental, 2016, 189: 172-180.

[46] Kim B, Hillman F, Ariyoshi M, et al. Effects of composition of the micro porous layer and the substrate on performance in the electrochemical reduction of CO_2 to CO[J]. Journal of Power Sources, 2016, 312: 192-198.

[47] Li F W, Thevenon A, Rosas-Hernandez A, et al. Molecular tuning of CO_2-to-ethylene conversion[J]. Nature, 2019, 577 (7791): 509-513.

[48] Singh M R, Kwon Y, Lum Y, et al. Hydrolysis of electrolyte cations enhances the electrochemical reduction of CO_2 over Ag and Cu[J]. Journal of the American Chemical Society, 2016, 138(39): 13006-13012.

[49] Li Q Y, Shi F, Shen F X, et al. Electrochemical reduction of CO_2 into CO in N-methyl pyrrolidone/tetrabutylammonium perchlorate in two-compartment electrolysis cell[J]. Journal of Electroanalytical Chemistry, 2016, 785: 229-134.

反应条件对铜催化 CO_2 电还原的影响

朱 畅[1,2],陈 为[1*],宋艳芳[1],董 笑[1],李桂花[1],魏 伟[1,3*],孙予罕[1,3*]

(1. 中国科学院上海高等研究院,中国科学院低碳转化科学与工程重点实验室,上海 201210;
2. 中国科学院大学,北京 100049;3. 上海科技大学物质科学与技术学院,上海 201210)

摘要: 工业规模的化石能源消耗导致大气中二氧化碳含量不断增加,CO_2 转化利用成为人们日益关注的热点问题. 金属铜因其成本低廉、储量丰富,并且具有独特的 CO_2 亲和力能够生成多碳化合物,是目前 CO_2 电还原中研究最为广泛深入的电极材料. 由于阴、阳离子的特征吸附对 Cu 电极性能有显著影响,并且不同反应体系中对 Cu 电极上 CO_2 吸附、活化影响也有所不同,因此导致金属 Cu 电极上报道的电催化活性、产物种类与选择性等都非常宽泛. 基于此, 有必要系统地研究各种反应条件对金属 Cu 电极电催化 CO_2 还原性能的影响. 作者选择了平均粒径为 600 nm 的商品化金属 Cu 颗粒作为电还原 CO_2 的催化剂, 研究了不同反应条件包括各种常用电解质溶液、$KHCO_3$ 的浓度以及 H 型电解池和流动池. 实验结果表明,浓度为 0.5 mol·L^{-1} 的 $KHCO_3$ 作为电解质溶液具有较好催化活性和较高的产物分电流密度,流动池可以进一步提高主要产物甲酸盐和 CO 的分电流密度. 本研究工作从反应条件的角度对 CO_2 还原的电催化转化进行了系统研究,有助于理解电解液和反应器等因素对 CO_2 电还原反应过程的影响规律.

关键词: 二氧化碳电还原;铜催化剂;反应条件;气体扩散电极